nature geoscience

LETTERS

PUBLISHED ONLINE: 31 OCTOBER 2016 | DOI: 10.1038/NGEO2828

Impact of decadal cloud variations on the Earth's energy budget

Chen Zhou*, Mark D. Zelinka and Stephen A. Klein

Feedbacks of clouds on climate change strongly influence the magnitude of global warming[1–3]. Cloud feedbacks, in turn, depend on the spatial patterns of surface warming[4–9], which vary on decadal timescales. Therefore, the magnitude of the decadal cloud feedback could deviate from the long-term cloud feedback[4]. Here we present climate model simulations to show that the global mean cloud feedback in response to decadal temperature fluctuations varies dramatically due to time variations in the spatial pattern of sea surface temperature. We find that cloud anomalies associated with these patterns significantly modify the Earth's energy budget. Specifically, the decadal cloud feedback between the 1980s and 2000s is substantially more negative than the long-term cloud feedback. This is a result of cooling in tropical regions where air descends, relative to warming in tropical ascent regions, which strengthens low-level atmospheric stability. Under these conditions, low-level cloud cover and its reflection of solar radiation increase, despite an increase in global mean surface temperature. These results suggest that sea surface temperature pattern-induced low cloud anomalies could have contributed to the period of reduced warming between 1998 and 2013, and offer a physical explanation of why climate sensitivities estimated from recently observed trends are probably biased low[4].

Clouds play a significant role in the Earth's climate system by reflecting incoming solar radiation and reducing outgoing thermal radiation. As the Earth's surface warms, the net radiative effect of clouds also changes, contributing a feedback to the climate system.

Recent studies suggest that the magnitude of climate feedbacks depends on surface warming patterns[4–9]. Therefore, we expect that the magnitude of decadal cloud feedback deviates from the long-term cloud feedback due to decadal variations in the spatial pattern of sea surface temperature (SST) anomalies[4], and may play a non-negligible role in decadal climate variability[10]. In this study, we perform idealized experiments to gain insight into the causes of decadal cloud variations over the past century. We then test the robustness of our experimental results by examining cloud trends during the satellite era in Coupled Model Intercomparison Project Phase 5 (CMIP5)[11] Atmospheric Model Intercomparison Project (AMIP) simulations, CMIP5-historical simulations, and observations.

Our experiments employ the Community Earth System model V1.2.1- Community Atmospheric Model 5.3 (CESM1.2.1-CAM5.3)[12] with a resolution of 1.9° longitude by 2.5° latitude. The control experiments ('AMIP-like', two runs with different initial conditions) use prescribed historical SST and climate forcings (aerosols, greenhouse gases, and solar radiation). To isolate the SST-driven component of cloud changes[4,7], we run two idealized 'AMIPFF' experiments with historical SST but climate forcings fixed at pre-industrial and present day levels, respectively. To investigate the effect of spatial patterns of SST anomalies on clouds, two patterned SST (PSST) experiments are carried out. The PSST experiments are identical to the AMIPFF experiments except that spatially uniform SST anomalies are subtracted from the historical SST at each time step to keep the global surface temperature roughly constant (see Methods). Historical sea ice is prescribed in all simulations. Confidence in CAM's simulation comes from its consistency with observations for the sensitivities of low cloud cover (LCC) to SST and estimated inversion strength (EIS)[13] and the recent evolution of cloud-controlling factors and cloud-induced radiation anomalies (Supplementary Figs 1–3).

Our analysis begins with the decadal net feedback (climate feedback parameter), which is calculated as the regression slope of annual global top of atmosphere (TOA) net flux anomalies against annual global surface temperature anomalies in AMIPFF simulations over 30-year windows[4]. Figure 1a indicates that the 30-year feedback parameter varies dramatically and is significantly more negative than the long-term net feedback (see Methods) after 1980. This is consistent with HadGEM2A/HadCM3A simulations carried out by Gregory and Andrews[4] and with experiments we have conducted with CAM4 (Supplementary Fig. 4), indicating that the decadal variations of net feedback are robust.

The variation of decadal net feedback is primarily induced by clouds (Fig. 1b and Supplementary Fig. 5). Decadal cloud-induced radiation anomalies ($\Delta R_{\mathrm{cloud}}$, see Methods) vary dramatically throughout the AMIPFF simulations while the global surface temperature increases relatively steadily (Fig. 2a), resulting in variations of decadal cloud feedback (Fig. 1b) and the corresponding net feedback. To understand the causes of decadal R_{cloud} variations, we decompose the cloud-induced radiation anomalies using the following equation

$$\Delta R_{\mathrm{cloud}} = \lambda_{\mathrm{c}} \Delta T_{\mathrm{s}} + \Delta R_{\mathrm{PSST}} + \Delta R_{\mathrm{cf}} + \varepsilon \quad (1)$$

where λ_{c} is the magnitude of cloud feedback under uniform SST warming (see Methods), T_{s} is global surface skin temperature, ΔR_{PSST} is the cloud-induced radiation anomaly in response to changes in SST pattern in the absence of global mean temperature changes ($=\Delta R_{\mathrm{cloud}}$ from PSST simulation), ΔR_{cf} is the rapid cloud radiative adjustment in response to changes in climate forcings (zero in our fixed forcing experiments), and ε is the error term. $\Delta R_{\mathrm{cloud}}$ in the AMIPFF simulation is well correlated ($r = 0.93$) with the sum of the $\lambda_{\mathrm{c}} \Delta T_{\mathrm{s}}$ and ΔR_{PSST} terms (Fig. 2a). These results suggest that cloud feedback can be linearly decomposed into a fixed feedback under uniform warming, plus a SST pattern-induced component.

Figure 2b shows the decadal anomalies in global LCC, which are primarily contributed from ΔLCC over the tropical oceans (Fig. 2c). The tropical marine ΔLCC in AMIPFF simulations is well correlated with and contributes significantly to variability in

Cloud Processes Research Group, Lawrence Livermore National Laboratory, Livermore, California 94550, USA. *e-mail: czhou.atmo@gmail.com

© 2016 Macmillan Publishers Limited, part of Springer Nature. All rights reserved.

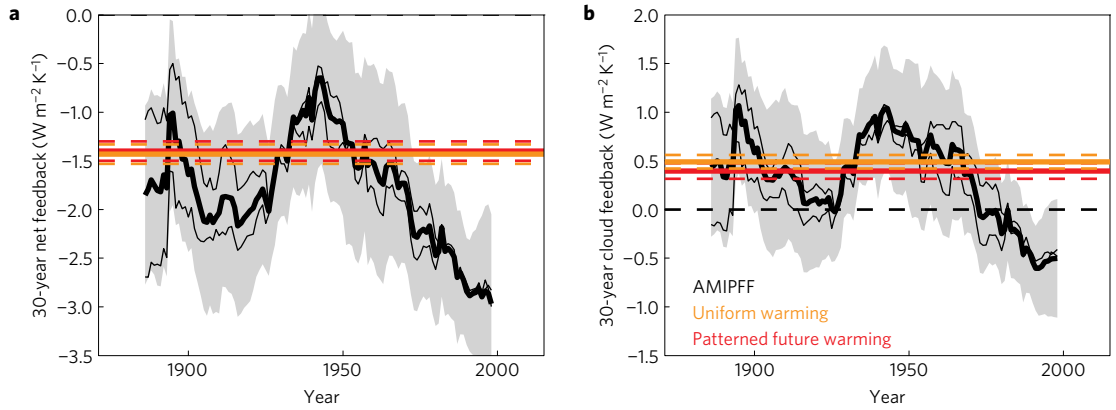

Figure 1 | Evolution of decadal net and cloud feedbacks from CAM5.3 simulations. a, Shown are the 30-year net feedback estimates from AMIPFF simulations, plotted at the midpoint of each 30-year period. Thin black lines are calculated from individual runs, and thick black lines are calculated from ensemble mean values. Horizontal solid lines denote the long-term cloud feedbacks computed from uniform (orange) and patterned (red) future warming experiments (see Methods). Dashed red/orange lines and grey shading denote 2σ uncertainty intervals. **b**, Same as **a**, but for the cloud feedback.

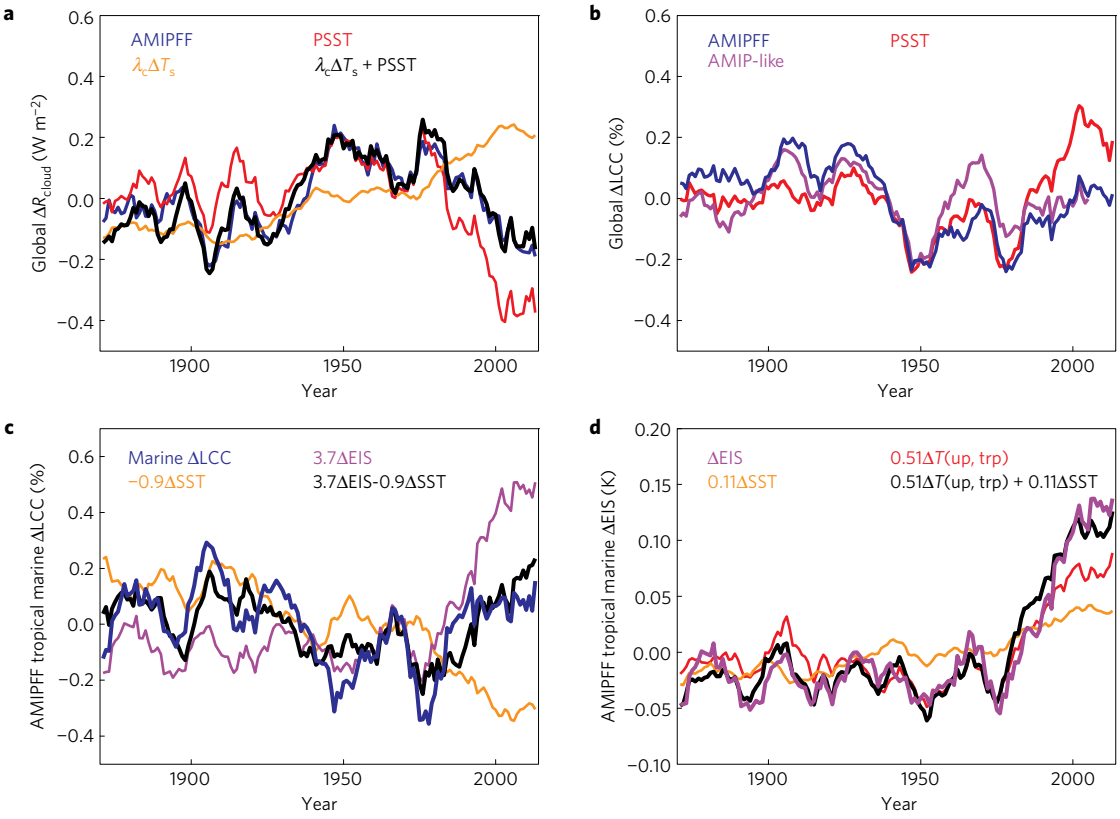

Figure 2 | Evolution of selected nine-year moving averaged quantities from CAM5.3 simulations. a, Global cloud-induced radiation anomaly in AMIPFF simulations (blue), its components due to anomalies in PSST (red) and global mean surface temperature (orange), and their sum (black). **b**, Global low cloud cover anomalies (ΔLCC) in all simulations. **c**, Tropical marine ΔLCC in AMIPFF simulations (blue), its components due to estimated inversion strength anomalies (ΔEIS) (purple), ΔSST (orange), and their sum (black). **d**, Tropical marine ΔEIS in AMIPFF simulations (purple), its components due to ΔT(up, trp) (red, see Methods), ΔSST (orange), and their sum (black).

the global ΔR_{cloud} ($r = -0.77$). These low clouds strongly cool the Earth's climate system and play an important role in determining the magnitude of cloud feedback[9,14–16].

We explain tropical marine ΔLCC with cloud-controlling factors. An increase in EIS or decrease in SST would contribute positively to LCC[9,16–18], so tropical ΔLCC can be explained by the linear combination of tropical mean SST and EIS anomalies (Fig. 2c, $r = 0.76$), with EIS anomalies explaining more decadal variance in LCC. Furthermore, changes in EIS are well explained ($r = 0.94$) by a linear combination of the tropical mean SST[19] and the difference between SST in tropical strong ascent regions and the tropical mean SST (ΔT(up, trp), see Methods), with the latter explaining more decadal variance in EIS (Fig. 2d). Physically, EIS increases with this SST difference because free-tropospheric temperatures throughout the tropics are controlled by the moist adiabat set by the SST in tropical ascent regions[20], whereas SSTs in tropical descent regions affect the temperature of boundary layer only locally. As a result, LCC variations over the twentieth century are primarily

© 2016 Macmillan Publishers Limited, part of Springer Nature. All rights reserved.

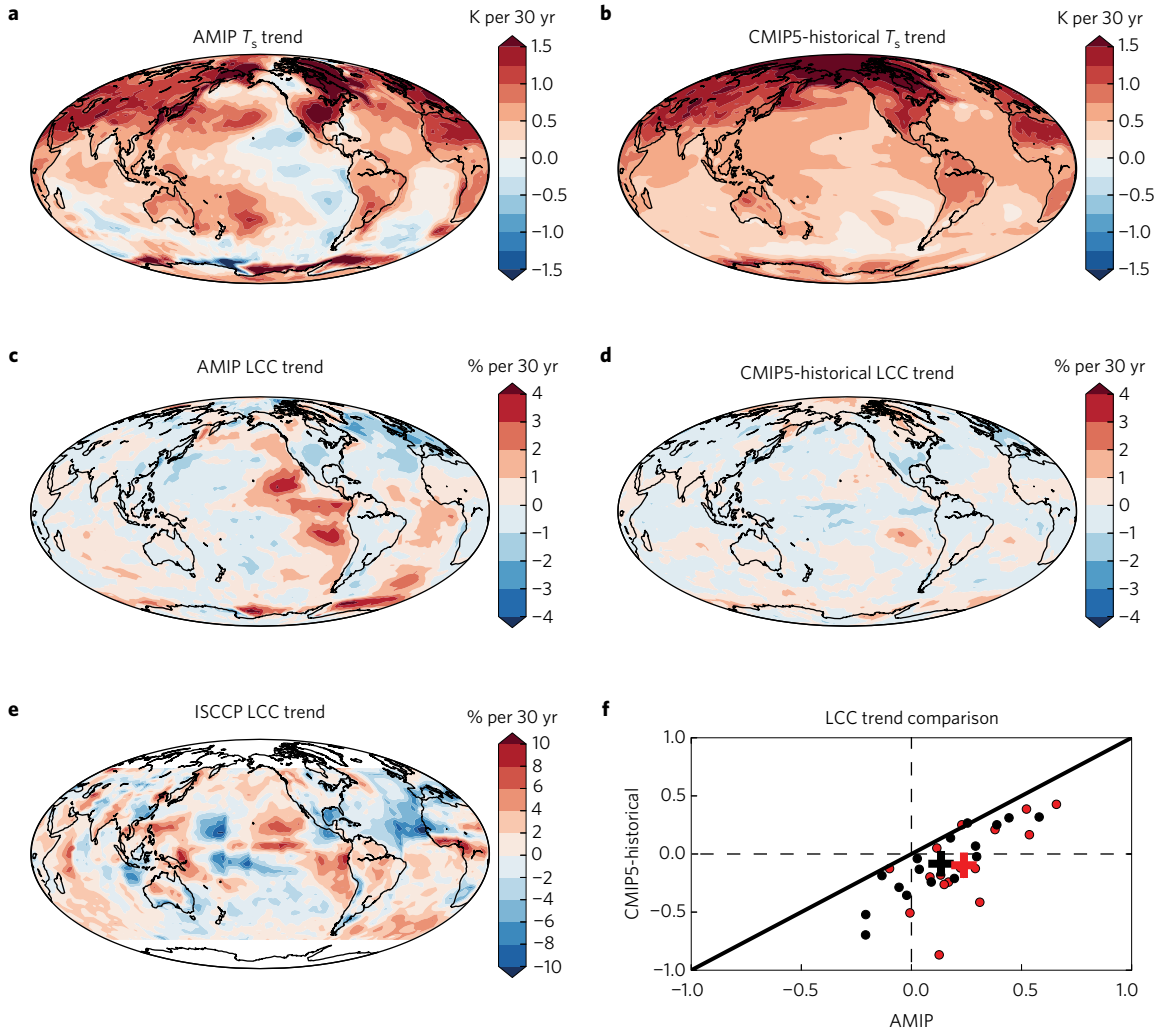

Figure 3 | Comparison of recent T_s and LCC trends in AMIP (1980–2005), CMIP5-historical (1980–2005) and satellite observations (1983–2005). **a**–**d**, Ensemble mean surface temperature and LCC trend in AMIP (**a**,**c**) and CMIP5-historical (**b**,**d**) simulations. **e**, LCC trend calculated from artefact-corrected International Satellite Cloud Climatology Project (ISCCP) satellite data[21,22]. Note that the colour bar in **e** is different from **c** and **d**. **f**, AMIP LCC trends plotted against CMIP5-historical LCC trends, for tropical (red) and global (black) averages, respectively (% per 30 yr). The solid black line is the equal-value line, and crosses denote model ensemble mean values.

induced by the SST pattern instead of changes in tropical mean SST (Supplementary Text 1 and Supplementary Fig. 6).

The above mechanism explains the abnormal decadal net feedback during the satellite era (1979-present), when surface warming is most pronounced over tropical ascent regions where deep convection occurs, with cooling over tropical descent regions, particularly in the Eastern Pacific where low clouds are common (Supplementary Fig. 7). The pronounced warming in the tropical ascent regions causes the tropical troposphere to warm and, in the absence of equivalent warming in descent regions, causes the tropical EIS to increase significantly (Fig. 2d), contributing positively to the LCC trend. Meanwhile, the SST-induced LCC reduction over the broader tropical oceans is not strong enough to compensate the EIS-induced LCC increase (Fig. 2c). Altogether, the positive tropical mean LCC trend results in a negative R_{cloud} trend (Fig. 2a), and hence a negative decadal cloud feedback during this period (Fig. 1b) because the negative R_{cloud} trend happens concurrently with a positive global mean surface temperature trend. SST, EIS, LCC and R_{cloud} trends also exhibit a clear spatial correspondence, confirming the physical linkages among them (Supplementary Fig. 8). As a result, the recent decadal feedback parameter is significantly more negative than the values under uniform or patterned long-term warming (Fig. 1a)[4].

To further demonstrate the importance of the SST pattern in driving LCC trends, we compare 1980–2005 LCC trends in AMIP with those in CMIP5-historical simulations (Supplementary Table 1). This comparison is valid because historical climate forcings are identically prescribed in both AMIP and CMIP5-historical simulations, meaning that differences are primarily the result of differing patterns of SST change between AMIP and CMIP5-historical simulations. In AMIP simulations, where the SST is the same as observations by design, there is significant LCC increase in the Eastern Pacific Ocean, Southern Indian Ocean, and Southern Atlantic Ocean (Fig. 3a,c), qualitatively consistent with artefact-corrected satellite observations[21,22] (Fig. 3e and Supplementary Fig. 9). In contrast, SST warming is distributed more uniformly in CMIP5-historical (Fig. 3b and Supplementary Fig. 10), and the model ensemble mean LCC trend is negative over much of the tropical regions (Fig. 3d). Averaging tropically or globally (Fig. 3f), the model ensemble mean LCC trend is positive in AMIP simulations, consistent with our CAM5.3 simulations, and negative in CMIP5-historical simulations, consistent with LCC changes under uniform and patterned long-term global warming (Supplementary Fig. 11). These differences hold for individual models as well: compared to historical simulations, the ΔT(up, trp) trend is

© 2016 Macmillan Publishers Limited, part of Springer Nature. All rights reserved.

systematically larger and the SST trend in descent regions is systematically smaller in AMIP simulations (Supplementary Fig. 12), leading to systematically more positive EIS and LCC trends in AMIP than in historical simulations (Fig. 3f). Examination of climate model control simulations suggests that these systematic differences may not be explained purely by lack of synchronization between internally generated trends in coupled historical simulations and those occurring in nature (Supplementary Text 2 and Supplementary Fig. 13). If so, the 1980–2005 SST trend pattern is likely to be partly forced, with a potentially important role for aerosols[23,24]. On the other hand, if models collectively underestimate internal variability on decadal timescales, the possibility remains that the pattern was an unusual natural fluctuation that coupled models do not simulate.

The average SST pattern-induced component of $\Delta R_{\mathrm{cloud}}$ is $-0.35\,\mathrm{W\,m^{-2}}$ during the 2000s (Fig. 2a), which is comparable to current TOA net flux anomaly ($\sim 0.6\,\mathrm{W\,m^{-2}}$)[25]. To the extent that the global warming rate is affected by the TOA net flux imbalance[26], SST pattern-induced negative R_{cloud} anomalies—together with oceanic heat storage at depth[23] and aerosol forcing[27,28]—are likely to have contributed to the global warming hiatus in the 2000s.

In conclusion, SST pattern-induced cloud anomalies have an important impact on the Earth's energy budget. Until the signal of greenhouse-gas-induced warming dominates over the noise of internal variability, the SST pattern-induced cloud radiation anomalies will be at least as large as those that are due to global surface warming. Indeed, SST pattern-induced enhancements in cloud cooling have dominated over the past several decades in CAM5.3 despite it having a positive cloud feedback under long-term warming. The SST trend pattern over the past three decades exhibits much greater warming in tropical ascent regions relative to the broader tropics, in contrast to the more uniform warming that characterizes observed long-term (1871–2005) SST trends, nearly all historical simulations between 1980 and 2005, and future projections of CO_2-induced climate change (Supplementary Figs 7 and 10). Therefore, both the cloud feedback and net feedback computed from recent trends are much more negative than in response to long-term warming, indicating that climate sensitivity estimated from recent climate changes is likely to be underestimated if SST pattern-induced cloud anomalies are not accounted for.

Methods

Methods, including statements of data availability and any associated accession codes and references, are available in the online version of this paper.

Received 27 May 2016; accepted 27 September 2016; published online 31 October 2016

References

1. Dufresne, J.-L. & Bony, S. An assessment of the primary sources of spread of global warming estimates from coupled atmosphere–ocean models. *J. Clim.* **21,** 5135–5144 (2008).
2. Webb, M. J. *et al*. On the contribution of local feedback mechanisms to the range of climate sensitivity in two GCM ensembles. *Clim. Dynam.* **27,** 17–38 (2006).
3. Caldwell, P. M., Zelinka, M. D., Taylor, K. E. & Marvel, K. Quantifying the sources of intermodel spread in equilibrium climate sensitivity. *J. Clim.* **29,** 513–524 (2016).
4. Gregory, J. M. & Andrews, T. Variation in climate sensitivity and feedback parameters during the historical period. *Geophys. Res. Lett.* **43,** 3911–3920 (2016).
5. Xie, S.-P., Kosaka, Y. & Okumura, Y. M. Distinct energy budgets for anthropogenic and natural changes during global warming hiatus. *Nat. Geosci.* **9,** 29–33 (2016).
6. Armour, K. C., Bitz, C. M. & Roe, G. H. Time-varying climate sensitivity from regional feedbacks. *J. Clim.* **26,** 4518–4534 (2013).
7. Andrews, T. Using an AGCM to diagnose historical effective radiative forcing and mechanisms of recent decadal climate change. *J. Clim.* **27,** 1193–1209 (2014).
8. Andrews, T., Gregory, J. M. & Webb, M. J. The dependence of radiative forcing and feedback on evolving patterns of surface temperature change in climate models. *J. Clim.* **28,** 1630–1648 (2015).
9. Zhou, C., Zelinka, M. D., Dessler, A. E. & Klein, S. A. The relationship between interannual and long-term cloud feedbacks. *Geophys. Res. Lett.* **42,** 10463–10469 (2015).
10. Brown, P. T., Li, W., Li, L. & Ming, Y. Top-of-atmosphere radiative contribution to unforced decadal global temperature variability in climate models. *Geophys. Res. Lett.* **41,** 5175–5183 (2014).
11. Taylor, K. E., Stouffer, R. J. & Meehl, G. A. An overview of CMIP5 and the experiment design. *Bull. Am. Meteorol. Soc.* **93,** 485–498 (2012).
12. Neale, R. B. *et al*. *Description of the NCAR Community Atmosphere Model (CAM 5.0)* NCAR/TN-486+STR (National Centre for Atmospheric Research, 2012)
13. Wood, R. & Bretherton, C. S. On the relationship between stratiform low cloud cover and lower-tropospheric stability. *J. Clim.* **19,** 6425–6432 (2006).
14. Bony, S. & Dufresne, J. L. Marine boundary layer clouds at the heart of tropical cloud feedback uncertainties in climate models. *Geophys. Res. Lett.* **32,** L20806 (2005).
15. Soden, B. J. & Vecchi, G. A. The vertical distribution of cloud feedback in coupled ocean–atmosphere models. *Geophys. Res. Lett.* **38,** L12704 (2011).
16. Sherwood, S. C., Bony, S. & Dufresne, J.-L. Spread in model climate sensitivity traced to atmospheric convective mixing. *Nature* **505,** 37–42 (2014).
17. Qu, X., Hall, A., Klein, S. A. & DeAngelis, A. M. Positive tropical marine low-cloud cover feedback inferred from cloud-controlling factors. *Geophys. Res. Lett.* **42,** 7767–7775 (2015).
18. Bretherton, C. S. & Blossey, P. N. Low cloud reduction in a greenhouse-warmed climate: results from Lagrangian LES of a subtropical marine cloudiness transition. *J. Adv. Model. Earth Syst.* **6,** 91–114 (2014).
19. Qu, X., Hall, A., Klein, S. A. & Caldwell, P. M. The strength of the tropical inversion and its response to climate change in 18 CMIP5 models. *Clim. Dynam.* **45,** 375–396 (2015).
20. Sobel, A. H., Nilsson, J. & Polvani, L. M. The weak temperature gradient approximation and balanced tropical moisture waves. *J. Atmos. Sci.* **58,** 3650–3665 (2001).
21. Seethala, C., Norris, J. R. & Myers, T. A. How has subtropical stratocumulus and associated meteorology changed since the 1980s? *J. Clim.* **28,** 8396–8410 (2015).
22. Norris, J. R. & Evan, A. T. Empirical removal of artifacts from the ISCCP and PATMOS-x satellite cloud records. *J. Atmos. Ocean. Technol.* **32,** 691–702 (2015).
23. Watanabe, M. *et al*. Contribution of natural decadal variability to global warming acceleration and hiatus. *Nat. Clim. Change* **4,** 893–897 (2014).
24. Takahashi, C. & Watanabe, M. Pacific trade winds accelerated by aerosol forcing over the past two decades. *Nat. Clim. Change* **6,** 768–772 (2016).
25. Stephens, G. L. *et al*. An update on Earth's energy balance in light of the latest global observations. *Nat. Geosci.* **5,** 691–696 (2012).
26. Smith, D. M. *et al*. Earth's energy imbalance since 1960 in observations and CMIP5 models. *Geophys. Res. Lett.* **42,** 1205–1213 (2015).
27. Santer, B. D. *et al*. Volcanic contribution to decadal changes in tropospheric temperature. *Nat. Geosci.* **7,** 185–189 (2014).
28. Estrada, F., Perron, P. & Martinez-Lopez, B. Statistically derived contributions of diverse human influences to twentieth-century temperature changes. *Nat. Geosci.* **6,** 1050–1055 (2013).

Acknowledgements

The authors thank J. Norris for providing the corrected ISCCP and PATMOS-x data, and thank J. Gregory, A. Dessler, A. Hall, H. Su, X. Qu, C. Terai and A. DeAngelis for valuable discussions. This work was supported by the Regional and Global Climate Modeling Program of the Office of Science at the US Department of Energy (DOE) under the project 'Identifying Robust Cloud Feedbacks in Observations and Models' and was performed under the auspices of DOE by Lawrence Livermore National Laboratory under Contract DE-AC52-07NA27344. IM Release #LLNL-JRNL-692260.

Author contributions

C.Z. performed the analysis. C.Z. and M.D.Z. designed the experiments. S.A.K. proposed the cloud analyses. The paper was discussed and written by all authors.

Additional information

Supplementary information is available in the online version of the paper. Reprints and permissions information is available online at www.nature.com/reprints. Correspondence and requests for materials should be addressed to C.Z.

Competing financial interests

The authors declare no competing financial interests.

© 2016 Macmillan Publishers Limited, part of Springer Nature. All rights reserved.

Methods

To carry out the PSST experiment, we first calculate the monthly global surface skin temperature anomalies $\Delta T_s(t)$ in AMIPFF experiments. In our uniform warming experiment, 1 K of uniform SST warming would increase the global surface temperature by ~1.1 K in CAM5.3, so we subtract $\Delta T_s(t)/1.1$ from the historical SST for each month and each location, and use the modified SST as boundary conditions. Then ΔT_s in the PSST experiment is near zero over the whole period (Supplementary Fig. 14), but the SST pattern anomalies are identical to those in the AMIP simulations.

Additional experiments are designed to calculate cloud feedback under uniform and patterned long-term global warming. First, we fix the SST and climate forcings at year 2000, and run for 16 years. Then we increase the SST by 4 K uniformly and reset the initial conditions, and run for another 16 years. Then the cloud feedback under uniform warming (λ_c) was calculated as the ΔR_{cloud} difference normalized by surface temperature difference between the latter 15 years of the two simulations. λ_c is close to the cloud feedback under patterned long-term warming (Fig. 1b), which is calculated with the same method, except that the SST of year 2000 is warmed by the long-term warming pattern derived from the ensemble mean of abrupt $4\times CO_2$ simulations (Supplementary Fig. 7).

Cloud-induced radiation anomalies (ΔR_{cloud}) are calculated by removing cloud masking effects from cloud radiative effect anomalies using radiative kernels[29], where cloud radiative effect is defined as the difference in upwelling radiation between clear- and all-sky scenes. LCC in CAM5.3 simulations is calculated by the model using the model's level-by-level cloud fraction field and its cloud overlap assumption. For AMIP and CMIP5-historical simulations, LCC is approximated as the maximum cloud fraction between the surface and 680 hPa, which is useful for qualitative comparisons[9,30].

To calculate decadal anomalies, we first calculate annual anomalies by removing the climatological mean from annual mean values. Then a nine-year moving average is applied to filter out interannual signals.

In Fig. 2, ΔT(up, trp) is calculated as the surface temperature difference between SST averaged over tropical strong ascent regions and SST averaged over the entire tropics at each time step. Tropical strong ascent regions are defined as those with monthly 500 hPa vertical velocity magnitude $|\omega_{500}|$ exceeding the median $|\omega_{500}|$ in regions with $\omega_{500} < 0$. The coefficients of ΔEIS and ΔSST in Fig. 2c, and of ΔT(up, trp) and ΔSST in Fig. 2d, are derived from multiple linear regression.

Code availability. The CESM1.2.1-CAM5.3 source code was downloaded from the CESM official website http://www2.cesm.ucar.edu. The CAM5.3 simulation results and code used for the analyses of this study are available from the corresponding author upon request.

Data availability. The CMIP5-historical/AMIP data is available from the Earth System Grid - Center for Enabling Technologies (ESG-CET) website, http://pcmdi9.llnl.gov.

References

29. Soden, B. J. *et al*. Quantifying climate feedbacks using radiative kernels. *J. Clim.* **21,** 3504–3520 (2008).
30. Noda, A. T. & Satoh, M. Intermodel variances of subtropical stratocumulus environments simulated in CMIP5 models. *Geophys. Res. Lett.* **41,** 7754–7761 (2014).

© 2016 Macmillan Publishers Limited, part of Springer Nature. All rights reserved.